Science & Technology Facilities Council

Technical Report
RAL-TR-2012-021

Mitigation of the electromagnetic pulse in petawatt laser shots

JE Bateman, MJ Mead

December 2012

RAL Library
STFC Rutherford Appleton Laboratory
R61
Harwell Oxford
Didcot
OX11 0QX

Tel: +44(0)1235 445384
Fax: +44(0)1235 446403
email: libraryral@stfc.ac.uk

Science and Technology Facilities Council reports are available online at: http://epubs.stfc.ac.uk

ISSN 1358- 6254

MITIGATION OF THE ELECTROMAGNETIC PULSE IN PETAWATT LASER SHOTS

J.E.Bateman,

Science and Technology Facilities Council, Rutherford Appleton Laboratory, Harwell Science and Innovation Campus, Didcot, Oxfordshire, OX11 0QX, U.K.

M. J. Mead

Institute of Physics of the Academy of Science, Na Slovance 1999/2, 182 21 Prague 8, Czech Republic

21 July 2012

Abstract

A simple model for the charge pulse induced in a metallic surface by an approaching charge travelling at relativistic velocity is developed. It indicates that the incident charge produces strong stimulation in the bandwidth of the normal mode resonances of a typical laser target chamber chiefly in the last few centimetres of travel before the surface is reached. The Electro-Magnetic Pulse (EMP) experienced in petawatt laser shots is believed to be generated in this way by the stimulation of the chamber resonance modes by the relativistic electron pulse. This finding is used to propose that arresting the relativistic electrons in a poorly conducting material a distance of a few tens of centimetres away from the chamber wall could usefully reduce the EMP.

1. Introduction

The scientific case for the Extreme Light Infrastructure (ELI) is predicated on the ability of petawatt laser pulses delivered in picosecond pulses to generate high energy x-rays (>1MeV), energetic ion beams (e.g. protons >100MeV) and ultra-short (attosecond) light pulses as well as electron beams of multi-MeV energies. All of these processes are dependent on the primary production of very hot (>MeV) electrons in the primary plasma which escape from the target region in copious ($>10^{12}$) quantities. The findings in the work described in ref. [1] that the EMP is attributable to escaping electrons rather than the neutral radiations emitted by the plasma (e.g. UV, x-rays and secondary electron created by them in the chamber walls) imply that the EMP will be an inescapable fact in virtually all ELI applications and that strategies for mitigation and accommodation must be considered as part of the design process.

In ref. [1] a sophisticated modelling process for the interaction of the escaping electrons with the target chamber is described and good agreement is obtained with the measured radiofrequency (RF) spectrum measured by the probes in the TITAN target chamber. However, a physical understanding of the mechanisms is not readily available from this approach. In our previous report [2] we used some of their data to validate a simpler physical model which can perhaps be more helpful for conceiving possible mitigation measures. The need for such measures has been widely noted [3,4].

In reference [2] we concentrated on modelling the bunching (in time) of the fast electrons caused by their relativistic velocities and how this bunching matches to the resonant modes of the target chamber. In this study attention is directed to a model of the induced charge (current) pulse that a bunch of relativistic electrons generates in metal surfaces as it approaches. In the previous study [2] proposals for mitigation were directed at damping the RF resonances of the target chamber once stimulated by the pulse of relativistic electrons. In this report the modelling of the induction pulse points to a possible mechanism for significantly reducing the stimulation of the chamber structure by the electron pulse in a relatively simple manner, so attacking the EMP at source.

2. The Fast Electron Distributions

Energy balance studies using the Rutherford Appleton Laboratory (RAL) lasers have indicated that above a threshold intensity of ~10^{18} W/cm^2 approximately 30% of the laser pulse energy is transformed into the kinetic energy of fast (>0.1MeV) electrons. [5] Energy spectra of pulses in this intensity range have been published in the study described in ref. [1] in which a series of high energy laser shots were fired at a 12 micron thick silver target of a range of sizes with a constant pulse length (2ps) and a constant spot diameter (~20 microns) (pulse energy not specified precisely but ~100J). Analysis of the spectra from a series of target foils with areas varying from ~0.16mm^2 to 100mm^2 shows that the fast electron distribution approximates to the sum of two quasi-thermal distributions with temperatures of ~0.4MeV and ~15MeV with variations in the temperatures according to target area [2].

Reference [6] presents measurements made on the PHELIX laser of the angular distributions of the fast electrons from a series of shots made in similar conditions to those of reference [1] – peak intensity of 3 x 10^{19} W/cm^2 onto 20μm thick Cu foils 2mm x 2mm in area with a focal spot of 30 x 13μm and a pulse length of 0.5ps. In general the fast electron distributions are found to peak around the incident beam direction within a half angle of ~30^o.

The dictates of Special Relativity mean that the fast electrons bunch tightly in time as their velocity asymptotically approaches the luminal value (**c** = 0.2998m/ns). The following relations hold: β (=v/**c** where v is the particle velocity) = $\sqrt{(1-1/\gamma^2)}$ where $\gamma = (1 + T_e/m_e)$ where T_e is the electron kinetic energy in MeV and m_e is the electron rest mass expressed in MeV (0.511MeV). Thus at T_e = 1.022MeV, γ = 3 and β = 0.943 and all electrons above this energy travel with similar velocities, close to **c**. The consequence of this effect, when allied with the fact that all electrons start their flight with in a picosecond time frame is to cause tight bunching in time and space of the fast electrons. Figure 1 shows the time distributions of a notional bunch at various flight times from the target as calculated from an energy spectrum of reference [1] and figure 2 shows the corresponding spatial snapshots at various flight distances [2]. The width (in time) of the leading "spike" in the figures varies linearly with the flight distance. At a flight distance of 1m it is typically ~10ps and its magnitude was found to correlate with the EMP measured at the same time [2].

The work of reference [2] showed that the waveform of figure 1 is perfectly matched to stimulate the rich spectrum of resonant modes present in a metal cavity of the dimensions typically used for a laser target chamber. This report develops a model of the mechanism by which such stimulation can occur in order to seek possible methods of interrupting this process and (at least partially) suppressing the resultant EMP.

3. The Induction Pulse

The basic electrical situation as far as the fast electrons are concerned is a simple separation of charges where the heavy positive ions in the laser-generated plasma do not move on the timescales of interest (~1ns) while the electrons fly off at near luminal velocities. This is analogous to the situation in a gas avalanche detector (with the polarities reversed) but with a dramatic distinction caused by the relativistic velocities of the electrons – namely that the dipole field generated initially propagates out to the chamber walls at a velocity only slightly greater than that of the electrons. (In the gas counter case the charge travels at a velocity << **c** so that the induced charge on the walls has ample time to adjust and one has a quasi-static situation describable by simple electrostatic laws.) Thus the chamber walls receive very little warning of the approach of the electron cloud leading to an impulsive stimulation. This impulsive stimulation is made even more extreme by the relativistic distortion of the electric field of the travelling electrons. Figure 3 shows a polar diagram of the relativistic form factor of an electron at different kinetic energies. The compression of the electric field into the transverse plane clearly means that the interaction with the chamber wall will be correspondingly compressed in time and very impulsive.

In electrical terms this means that the magnitude of the charge/current instantaneously induced in the chamber walls (or any metal surface encountered) will be determined

by final approach of the electron cloud to the surface. A simple model of this situation has been developed which illustrates the effect and provides some quantitative estimates.

3.1 The Model

The charge density induced on an infinite conducting plane by an approaching charge e can be simply calculated by the method of image charges in which a pseudo-charge of -e is located on the opposite side of the plane and at the same distance as e. A coordinate system is chosen such that the line of approach of the charge is the –ve x-axis with the y and z axes mutually orthogonal within the plane. The symmetry of the situation dictates that the x component of the field due to e at any point on a circle of radius r ($=\sqrt{(y^2 + z^2)}$ is just twice the x component ($E_x(r)$) generated by e at the point. Gauss' Theorem now yields the relation:

$$\sigma(r) = 2\varepsilon_0 E_x(r) \qquad (1)$$

where ε_0 is the permittivity of free space and $\sigma(r)$ is the induced charge density.

Considering the charge **q** approaching at near-luminal velocity v located at x = -vt at time t the relativistic expression for the electric field of the charge must be used in place of the usual static field formula. This is: [7]

$$E_x(r) = \frac{e\gamma vt}{4\pi\varepsilon_0\left(\gamma^2(vt)^2 + r^2\right)^{3/2}} \qquad (2)$$

Substituting the expression for $E_x(r)$ from (2) into relation (1) gives the charge density on the plane arising from the approaching charge. Since the induced charge density is clearly circularly symmetric it is more informative to consider the radial charge density, i.e.

$$dq = \sigma(r)2\pi r dr$$

Thus finally:

$$dq = \frac{e\gamma vtr}{\left(\gamma^2(vt)^2 + r^2\right)^{3/2}} dr \qquad (3)$$

For our purposes this relation is more conveniently expressed with v in terms of γ:

$$dq = \frac{e(\gamma^2 - 1)^{1/2} ctr}{\left((\gamma^2 - 1)(ct)^2 + r^2\right)^{3/2}} dr \qquad (4)$$

Equation (4) clearly describes a radially symmetric distribution of induced charge. Figure 4 presents plots of this distribution (expressed as a fraction of the approaching charge **e**) at various times before impact. Since the charge velocity is nearly luminal

the approximate distance from impact is estimated as **c**t (x in the figure). As the charge approaches the plane the maximum of the charge distribution rises rapidly and converges on the origin (i.e. the point of impact).

Integrating equation (4) over the plane i.e. r = 0 to r = ∞ produces the result q = **-e** since an infinite plane will catch all the field lines from **e**. Thus to use equation (4) it is necessary to specify a value of r_{max}. This seems at first sight to require an arbitrary decision. However, the vessel of interest is of finite size and (more importantly) the very short timescales of relevance in this study (~1ns) mean that effectively the point of impact cannot receive information from distances greater than **c**t, i.e. about 0.3m. The integral of equation (4) from r = 0 to r = r_{max} is:

$$\Delta q = -e\left[1 - \frac{(\gamma^2 - 1)^{1/2} ct}{\left((\gamma^2 - 1)(ct)^2 + {r_{max}}^2\right)^{1/2}}\right] \qquad (5)$$

Figure 5 presents plots of the induced charge as a function of the time to impact within a circle of 0.5m diameter of the impact point as evaluated from equation (5) with the range of γ approximating to electron energies of 1MeV to 30MeV.

The model predicts that the charge impulse seen by the plane has a half width of <<1ns for all electron energies >1MeV. Increasing r_{max} increases the half width of the induction pulse. Figure 6 presents the plots for integration of equation (5) over a 1m diameter circle. However, it is doubtful if this is a meaningful choice for the fast electrons.

In reference [2] it was shown that the fast electrons have a quasi-thermal (i.e. negative exponential) energy distribution. In order to assess the effect of this distribution on the induced charge pulse a simple computer program was used to convolve a simple thermal electron energy spectrum into the induced charge formula (5). Figure 7 shows the results. The curves are in general less steep since the electron spectrum was continued down to energies of 0.05MeV. Figure 8 plots the half height times as a function of electron temperature as obtained from figure 7. There is an approximately linear relationship with half width times well below 1ns.

The model has been used to test the implications of the suggestion that as the intensity of the laser beam rises above the threshold for fast electron production a constant fraction (~30%) of the pulse energy is converted into fast electrons. Thus, as the pulse energy rises the temperature of the electron distribution rises proportionately and the number in the distribution remains approximately constant. Figure 9 illustrates the predictions of the model for the induction pulse waveform when the number of fast electrons is held constant while the temperature is scaled up by a factor of 10 (corresponding to a tenfold increase in laser pulse energy). The half width of the induction pulse reduces by a factor of 7.4 due to the higher electron energies so while the amplitude does not change the bandwidth is increased by the factor of 7.4 with negative consequences for the EMP.

The final conclusion of the model is that the mechanism of charge induction on the vessel and any metal within it is fast enough to preserve the sub-nanosecond impulse

structure of the electron cloud flight characteristics and trigger the fast E-M oscillation modes in the chamber vessel which characterise the EMP.

4. A Possible Strategy for Mitigation

All the plots of model induction pulses show that the fast electrons do not drive the highest currents into the metal of a surface until they are within tens of picoseconds of the surface i.e. a very few centimetres distant at near luminal velocity. This fact leads to the idea that stopping the fast electrons in a non-metallic material a suitable distance from any metal surface (a few tens of centimetres) may well be a viable strategy for reducing the EMP. The essential theoretical requirements for this stopping material are only two: a suitable, low bulk conductivity and adequate stopping power for the most energetic electrons.

The former requirement can be met by a wide variety of semiconducting or semi-insulating materials – a suitable range of bulk resistivity is approximately 10^3 to 10^9 ohm-cm. Materials in this range behave essentially as insulators as far as the incident fast electrons are concerned but have enough conductivity to complete the return circuit adequately. (Relativistic charged particles interact only very weakly with the boundary of an insulator. This weak radiation emitted is known as Transition Radiation).

The second requirement can be met in the case of electrons up to ~50MeV in energy by a few centimetres of solid material. A material with high atomic number (Z) will generally reduce the required thickness of absorber to less than 1cm in the 10MeV region. However, such a material has the side effect of generating gamma rays very efficiently from the fast electrons (via the Bremstrahlung process) and also photo-neutrons. Consequently it is wise to use materials of low Z which stop the fast electrons more cleanly.

In the practical situation important requirements remain such as, vacuum compatibility, availability, convenience of handling and cost. Silicon carbide (SiC) has been investigated as a possible candidate for this material. SiC is a low-Z semiconductor, the resistivity of which can be easily varied by doping over many orders of magnitude. It is an industrial material, readily and cheaply available as a refractory liner for furnaces and therefore likely to be very vacuum compatible. (The resistivity of such material is not controlled for that application and would require to be determined.) The relatively high density of SiC ($3.21 g/cm^3$) keeps down the thickness of material required to stop 50MeV electrons. Figure 10 shows the range energy curve of electrons in SiC as estimated from the calculations tabulated in reference [8]. These calculations use the Continuously Slowing Down Approximation (CSDA) to calculate the specific energy loss and hence the range. The range thus calculated is the actual path length followed by an electron. This path length is very much longer than the average distance travelled by the electron in the material due to the path being very much folded by the effects of multiple scattering. However, it does give a good estimate of the thickness of material required to block essentially all the electrons. Figure 10 shows that 7cm of SiC is required for the purpose of absorbing electrons up to 50MeV in energy.

Clearly, a wide choice of materials is potentially available to meet the requirements listed above – SiC is simply quoted as an example. However, studies undertaken at The National Laboratory for High Energy Physics in Japan [9], show that not only is commonly-available sintered SiC material very vacuum compatible but also has appropriate electrical characteristics as an RF absorber in the GHz frequency range. It was found that at 1GHz the loss tangent was 0.32 and the dielectric constant (real part) was 22. These numbers translate to a bulk resistivity of 225 ohm-cm, a suitable value for both the electron-stopping requirement and RF damping requirement.

5. Discussion

The effect on the induction pulse of arresting the burst of fast electrons in advance of its arrival at the chamber wall can be estimated from figure 7 which shows the induced charge as a function of the time to impact (t_i) for quasi-thermal electron distributions with temperatures from 1MeV to 32MeV. Since the electrons are essentially travelling at luminal velocity, stopping them at a distance of 30cm from the wall will mean that the induction curves of figure 7 will maximise at t_i = 1ns. For the 1MeV distribution this results in a reduction of a factor of ~5 in amplitude and for the 32MeV distribution a factor of >100. The second implication of figure 7 is that the bandwidth of the driving pulse is much reduced, especially in the case of higher energy distributions – for the 32Mev distribution it increases from ~10ps to 1ns.

Thus the potential benefit of the proposed electron absorber is twofold: both the amplitude and the bandwidth of the induced charge pulse are reduced. This proceeding will not eliminate the stimulation of the chamber but by shifting the frequency spectrum downwards will reduce the oscillatory modes available and improve the efficacy of an RF absorption strategy (as proposed in reference [2]) which can be used in combination with the electron absorber.

Acknowledgement

This work benefited from support of the ELI: Extreme Light Infrastructure OP VaVpI project No. CZ.1.05/1.1.00/02.006.

References.

1. Mitigation of Electromagnetic Pulse (EMP) Effects from Short-Pulse lasers and Fusion Neutrons, D C Eder, A Throop, C G Brown Jr., J Kimbrough, M L Stowell, D A White, P Song, N Back, A MacPhee, H Chen, W DeHope, Y Ping, B Maddox, J Lister, G Pratt, T Ma, Y Tsui, M. Perkins, D O'Brien and P Patel, LLNL-TR-411183 (2009).
2. Electromagnetic Pulse Generation in Petawatt Laser Shots, J E Bateman and M J Mead, RAL-TR-2012-005
3. Operation of target diagnostics in a petawatt laser environment, C Stoecki et. al., Rev. Sci. Instr. 77, 10F506 (2006).
4. New constraints for plasma diagnostics due to the harsh environment of MJ class lasers, J L Bourgade et. al., Rev. Sci. Instr. **75** (10) 4204, 2004.

5. D. Neely, Private communication.
6. R J Gray et. al. Applied Physics Letters 99, 171502 (2011)
7. E. Laing, Lectures on Special Relativity, Glasgow University 1962 (unpublished)
8. L. Pages et. al., Atomic Data **4**, 1 as tabulated in Kaye and Laby, Tables of Physical and Chemical Constants, Longmans (1995) pp409-410.
9. "Hom Absorber for the Kekb Normal Conducting Cavity, Y. Takeuchi, K. Akai, N. Akasaka, E. Ezura, T. Kageyama, F. Naito, T. Shintake, and Y. Yamazaki, KEK, National Laboratory for High Energy Physics, 1-1 Oho, Tsukuba, Ibaraki, 305 JAPAN

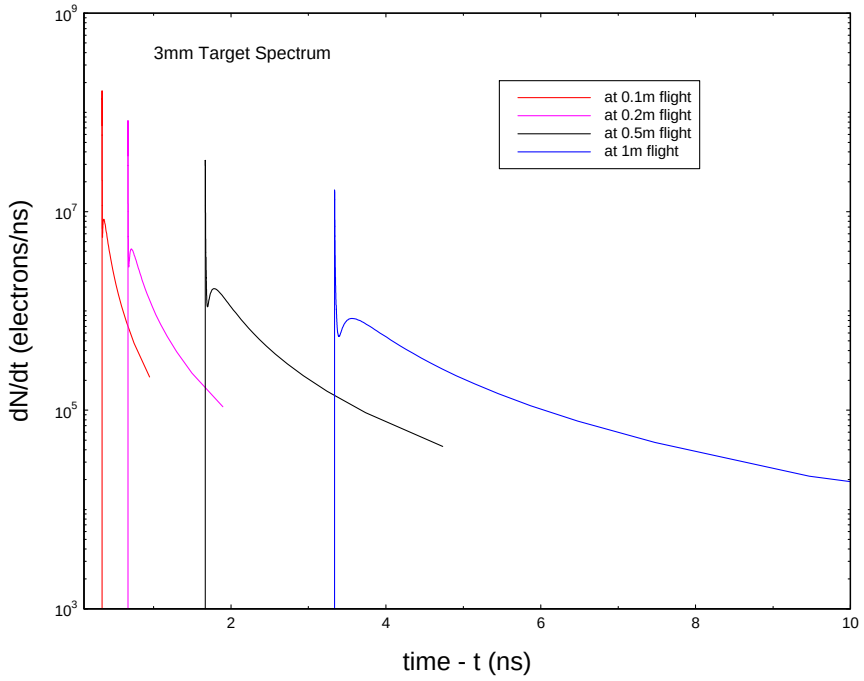

Figure 1. Time distributions of the electrons in the bunch at different flight distances

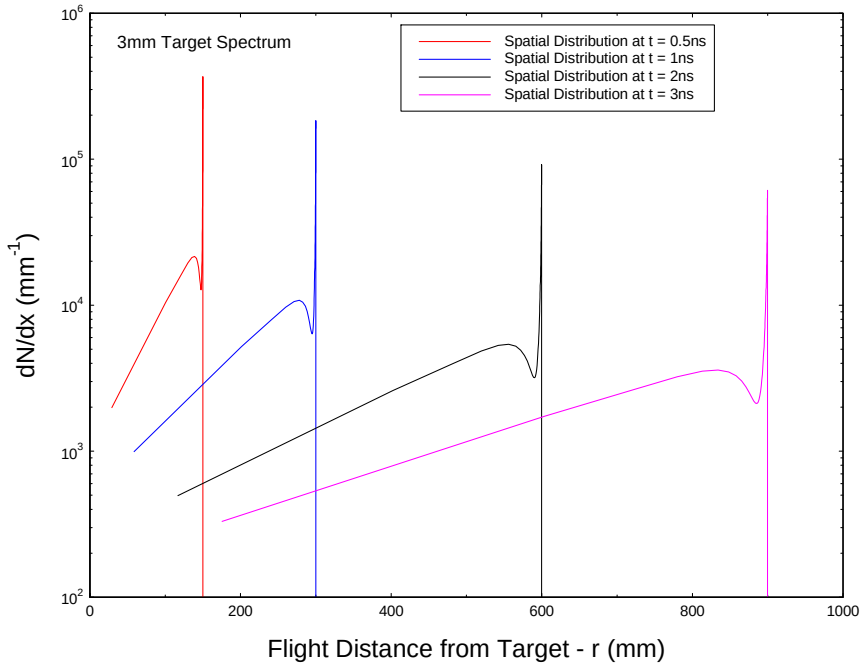

Figure 2. Electron bunch radial profiles at different flight times before wall impact

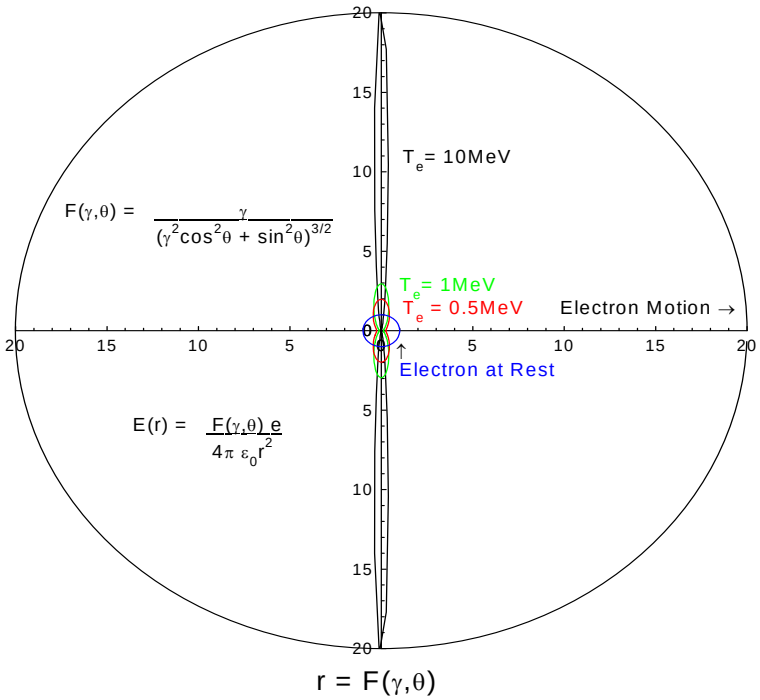

Figure 3. Polar plot of Relativistic Form Factor for the E field of a moving electron.

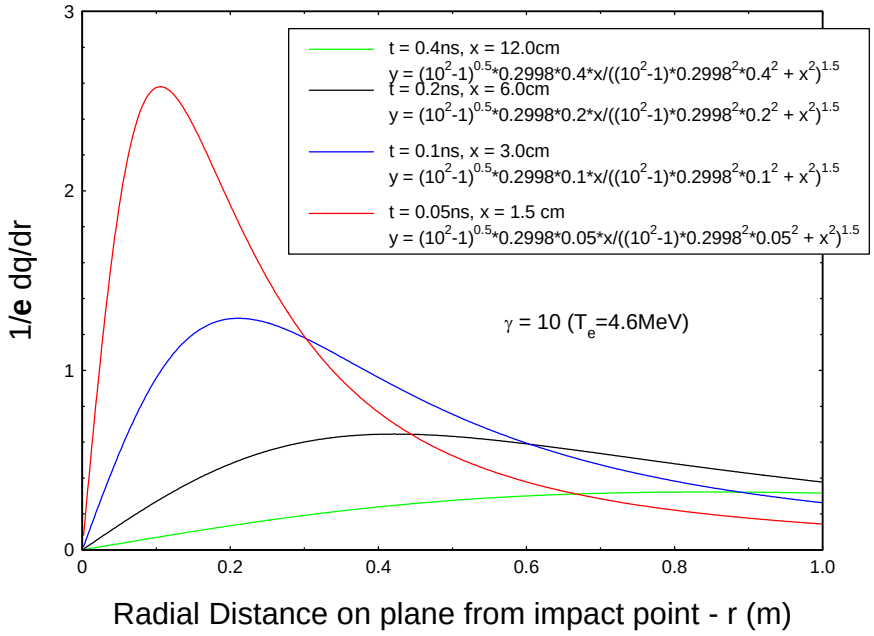

Figure 4. The radial distribution of the charge induced by an electron approaching a plane conducting surface.

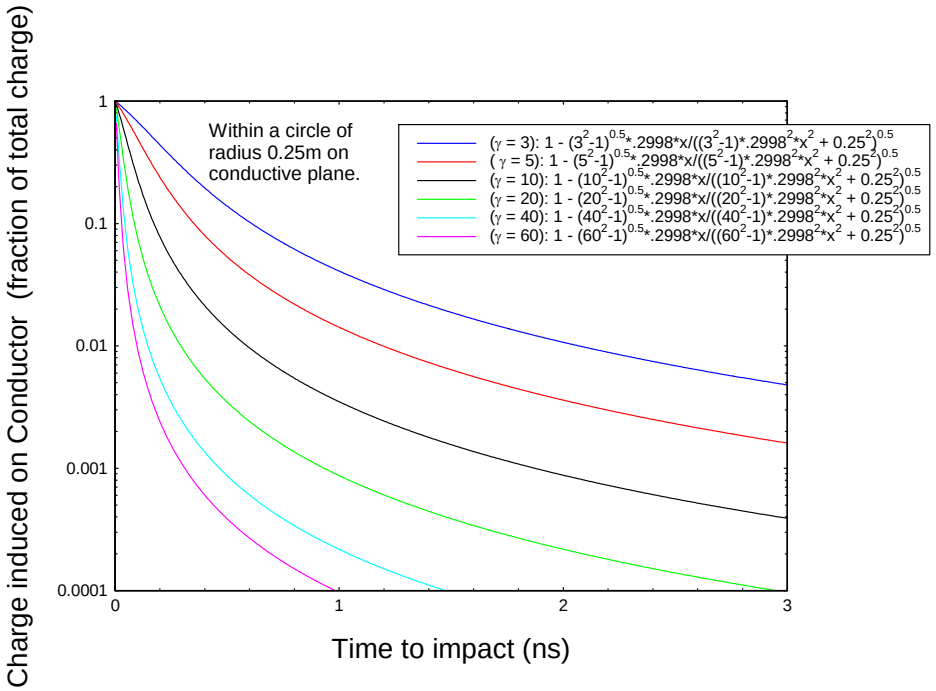

Figure 5. The fractional charge induced on a conducting plane by an approaching electron within a circle of 25cm radius from the impact point.

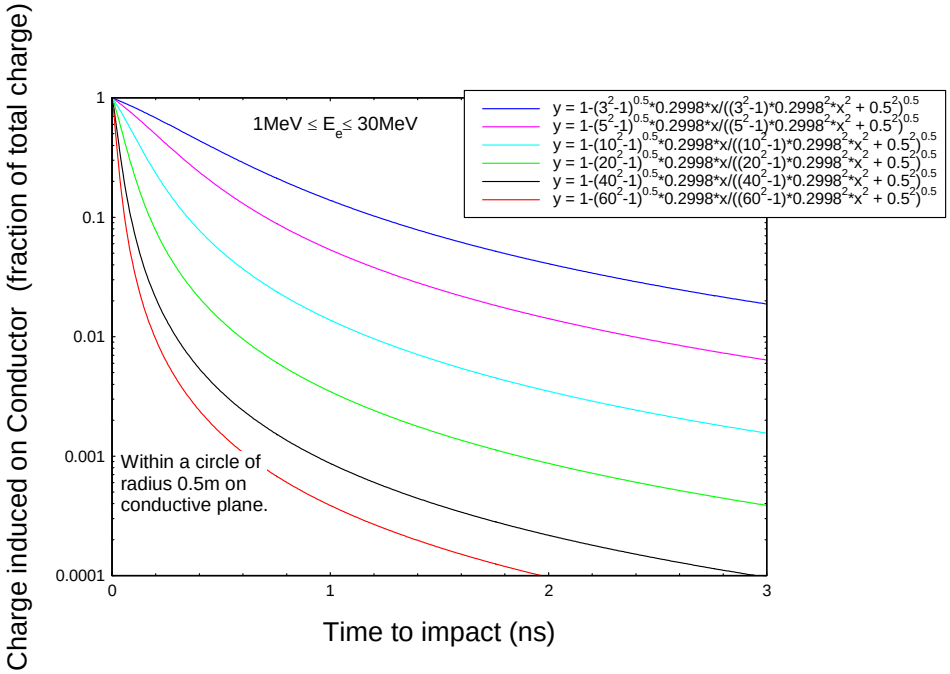

Figure 6. The fractional charge induced on a conducting plane by an approaching electron within a circle of 50cm radius from the impact point.

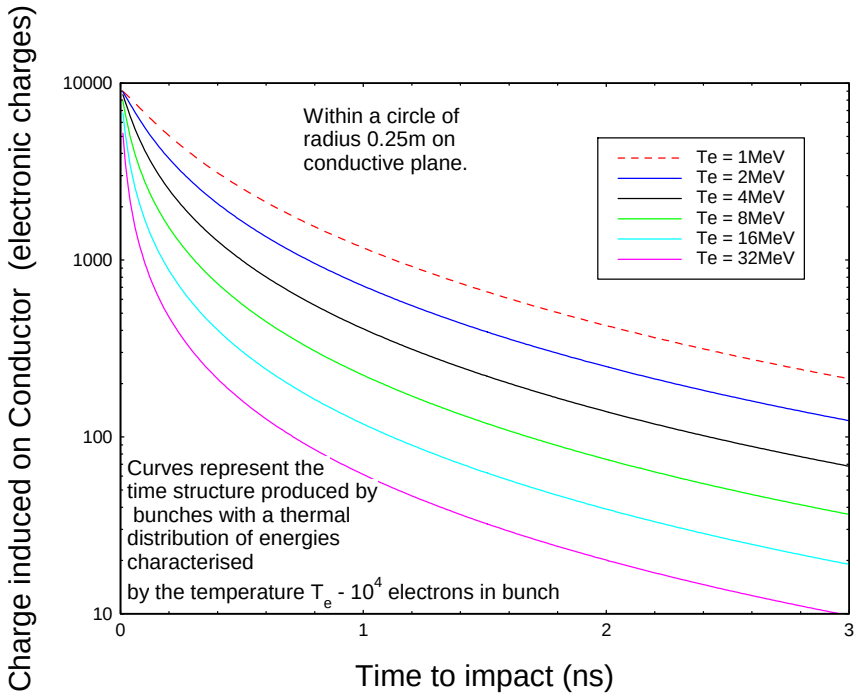

Figure 7. The charge induced on a conducting plane by an approaching electron bunch of 10^4 electrons with a quasi-thermal energy distribution within a circle of 25cm radius from the impact point.

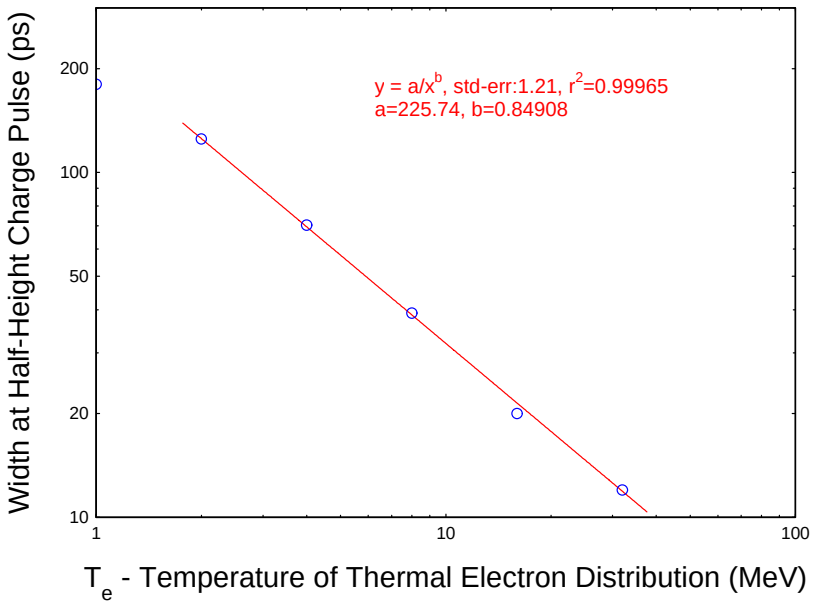

Figure 8. The width at half height (as a function of T_e) of the induction pulse curves of Figure 7.

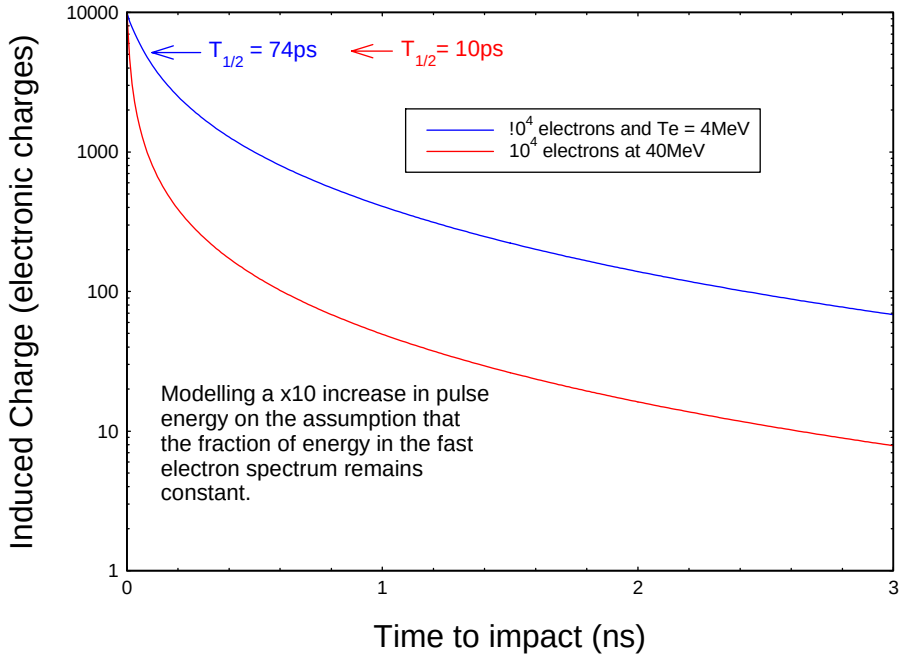

Figure 9. Simulating the effect of the constraint that the fraction of energy in the fast electron spectrum remains constant as the laser pulse increases.

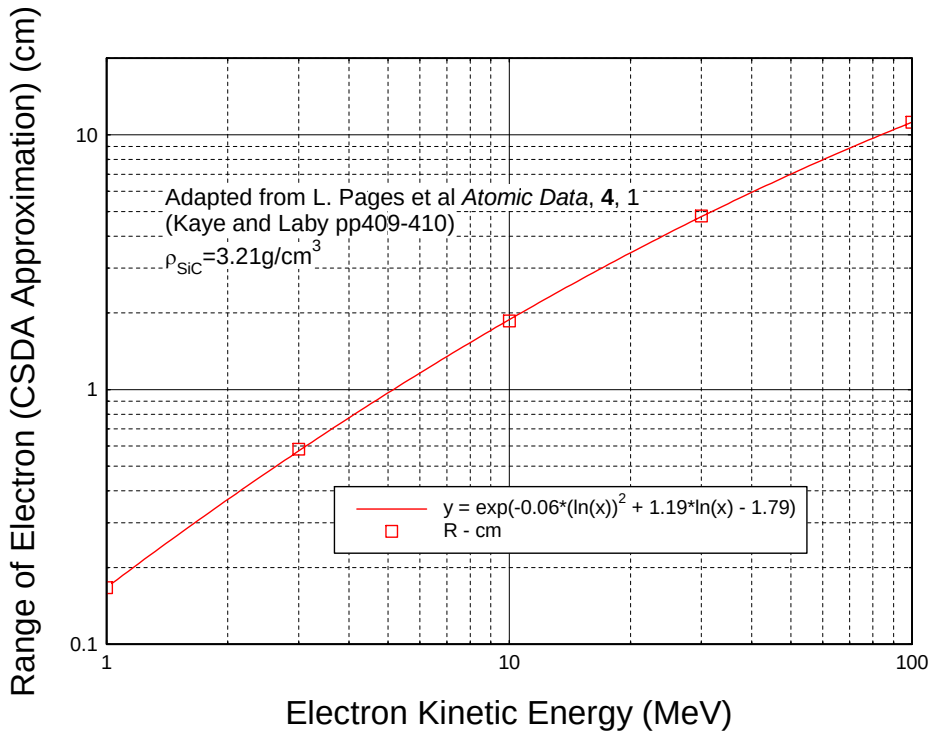

Figure 10. The estimated Range-Energy curve for fast electrons in SiC